Available online at www.sciencedirect.com
SCIENCE DIRECT
Polymer 46 (2005) 12256–12266
polymer
www.elsevier.com/locate/polymer

Introduction of long-chain branches in linear polyethylene by light cross-linking with 1,3-benzenedisulfonyl azide

J.K. Jørgensen [a,*], Aage Stori [b], Keith Redford [b], Espen Ommundsen [c]

[a] *Department of Engineering Design and Materials, Norwegian University of Science and Technology, Richard Birkelandsvei 2b, 7491 Trondheim, Trondheim, Norway*
[b] *SINTEF materials and chemistry pb. 124 Blindern, 01314 Oslo, Norway*
[c] *Bosealis ASIN-3960 Stathelle, Norway*

Received 28 February 2005; received in revised form 14 October 2005; accepted 17 October 2005
Available online 4 November 2005

Abstract

Metallocene synthesised HDPE with $M_w = 82{,}000$ and $M_n = 40{,}000$ was modified with small amounts of 1,3-benzenedisulfonyl azide by reactive extrusion at 200 °C with the purpose to form long-chain branches. At the processing temperature the two azide groups decompose to nitrenes that work as cross-linkers for PE. Cross-linking occurs primarily by insertion of singlet nitrenes into CH bonds. Size exclusion chromatography revealed that the modification resulted in the formation of a long-chain branched (LCB) high molecular weight fraction. The LCB was detectable with SEC for concentrations above 100 ppm corresponding to approximately 0.03–0.04 branch points pr 10^4 carbon. No signs of the formation of low molecular species due to chain scission were observed. Dynamical mechanical analysis and shear creep test showed sign of long chain branching at concentrations down to the same limit as SEC (100 ppm). These signs were thermorheological complexity, increased zero shear viscosity, increased shear thinning and increased recovery compliance. The cross-linking efficiency of 1,3-BDSA were estimated to 40–60% from comparison of SEC data with random cross-linking theory and traditional SEC-LCB analyses.

Keywords: Cross-linking; Long-chain branching; Sulfonyl azides

1. Introduction

Despite that all polyolefins are aliphatic hydrocarbons they show a large diversity in mechanical properties in both the solid and the melt state. This is due to differences in the molecular architecture. The molecular architecture is described by the molecular weight M_w, the molecular weight distribution (MWD) and the content and distribution of branches. Long-chain branches (LCB) are structural features that have large impact on the rheological (melt) properties. If the LCB are few and long they are crystallizable like linear chains and have small influence on the solid-state properties. An example of this is LCB-HDPE synthesized with metallocene catalysts. On the other hand the dendritic structure of traditional LDPE with both long and short branches leads to low crystallinity and solid state properties much different from a linear PE.

LCB can be incorporated directly during the synthesis, as is the case for traditional radical polymerised LDPE and modern metallocene catalysed qualities. Another approach is introduction of LCB by light cross-linking of linear polyolefins in a post reactor reaction. Cross-linking is normally done using peroxides, radiation or vinyl silanes. In this work light cross-linking with 1,3-benzenedisulfonyl azide (1,3-BDSA) has been used to introduce LCB in polyethylene. The use off 1,3-benzenedisulfonyl azide as a cross-linking agent in polyolefins and polyolefin containing blends is covered in a number of patents and publications [1–5] but to our knowledge very little [6,7] has been reported on the use of 1,3- BDSA to form LCB. The objective of this work has been to verify that light cross-linking with 1,3-benzenedisulfonyl azide can be used as a method to introduce LCB in linear polyethylene. This paper covers the modification of linear PE and characterisation of the modified samples with SEC, rheometry, melt flow index, gel content and density measurements.

1.1. Reactions of 1,3-BDSA with hydrocarbons

The chemical structure of 1,3-BDSA is shown in Fig. 1. The thermal decomposition of sulfonyl azides in organic solvents

* Present address: SINTEF materials and Chemistry pb. 124 Blindern, 0314 Oslo, Norway. Tel.: +47 98243957
E-mail address: jens.k.jorgensen@sintef.no (J.K. Jørgensen).

0032-3861/$ - see front matter © 2005 Elsevier Ltd. All rights reserved.
doi:10.1016/j.polymer.2005.10.084

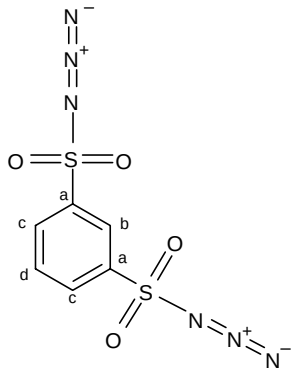

Fig. 1. Chemical structure of 1,3-benzenedisulfonyl azide.

and mineral oil have been studied in detail [8,9]. Recently we investigated the decomposition and reaction of 1,3-BDSA dissolved in a polyolefin [10]. At elevated temperatures sulfonyl azides decompose to form a sulfonyl nitrene as shown in reaction Scheme 1. The nitrene can exist in both the singlet and the triplet state. Both states can react with hydrocarbons but they do so in different ways. The reaction involving the singlet nitrene is an insertion at the C–H bond giving a secondary sulfonyl amide (Scheme 2). The triplet nitrene react by abstraction of a proton from the hydrocarbon resulting in the formation of a macroradical (Scheme 3(a)). This reaction can be followed either by a recombination of the two products to form the product of Scheme 3(b) or by abstraction of second proton from another hydrocarbon (Scheme 3(c)) to give a primary sulfonyl amide. Whether recombination or a second abstraction will occur depends on the mobility of the hydrocarbon. The amount of recombination decreases as the mobility of the hydrocarbon increases [11]. Earlier studies [10] have shown that the decomposition of 1,3-BDSA blended in a stabilized polyolefin melt is a first order reaction. Formation of singlet nitrenes, followed by insertion in the carbon chain, is the dominating reactions. Life times of 1,3-BDSA at different temperatures are listed in Table 1. With insufficient blending or in presence of oxygen other unwanted reactions can occur [10,12].

For the purpose of cross-linking the reactions of Schemes 2 and 3, (a+b) or (a+c) followed by macroradical recombination, have to occur. These reactions have to take place on both azide groups of 1,3-BSDA and with different polymers. The simplest branching structure rising from these reactions will be four armed stars with 1,3-BDSA as the centre point. The arm length will be dependent on the length of the two linear chains forming the star and the position of the cross-linking point

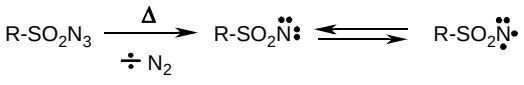

Scheme 1. Formation of singlet and triplet nitrenes from azide.

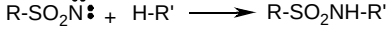

Scheme 2. Reaction of singlet nitrene with hydrocarbon. Formation of secondary sulfonyl amide.

Scheme 3. Reaction of triplet nitrene with hydrocarbon. (a) Formation macroradical by Habstraction. (b) Formation of secondary sulfonyl amide by recombination. (c) Formation of primary sulfonyl amide by abstraction of a second proton.

along these chains. Such a structure is expected to be dominant for a low concentration and even distribution of 1,3-BDSA in the polymer matrix. For high concentration of 1,3-BDSA or if local clusters of 1,3-BDSA exist more complex structures will also appear, but our earlier work [10] suggests that 1,3-BDSA can be evenly dispersed or dissolved in a polyolefin melt. Another possibility is loop structures formed if 1,3-BDSA connects to two carbons on the same chain.

1.2. Random cross-linking

With good blending of the sulfonyl azide into the polymer we can expect the cross-linking to be random. Simple equations have been derived for the evolution of the degree of polymerization averages during random cross-linking of linear precursors. The weight average degree of polymerization P_w is given by [13]

$$p_w = \frac{p_{wp}(1+\beta)}{1-(p_{wp}-1)\beta} \tag{1}$$

P_{wp} is the weight average degree of polymerization of the linear precursors and β is the cross-linking density defined as

$$\beta = \frac{\text{number of crosslinked monomers}}{\text{total number of monomers}} \tag{2}$$

In this connection one should note that one cross-link contains two cross-linked monomers. Eq. (1) has been derived under the assumptions that all monomers have the same probability to be cross-linked but that no intrachain cross-linking occurs. In the ideal case the number of cross-linked monomers should be the double of the number of cross-linkers. In reality the efficiency of the of the cross-linker ν can be described by some value between zero and one related to β as

$$\beta = \nu\frac{2\times\text{number of crosslinkers}}{\text{total number of monoments}} \tag{3}$$

Table 1
Half-lives and nine times half-lives of 1,3-BDSA in polyethylene Dow Affinity SQ1503 UE

Temperature (°C)	220	200	180	160
$t_{1/2}$ (s)	4.7	25.7	162	1209
$9\times t_{1/2}$ (min) (99.8% conversion)	0.71	3.8	24.3	181

Values taken from [10].

Hence ν can be estimated from $P_w/P_{wp} = M_w/M_{wp}$ where M_w and M_{wp} are weight molecular weight average of the cross-linked polymer and the linear precursors, respectively.

1.3. LCB and rheology

The rheology of polyolefin melts is very sensitive to LCB. A review on this has been given by Bubeck [14]. The origin for this lies in the ability of LCB-containing chains to form strong entanglements with their surrounding chains [14,15]. These entanglements lead to a more complicated relaxation pattern than the one found in linear materials. First of all entangled chains relax much slower than non-entangled chains. This broadens out the relaxation spectrum and makes the material more elastic both in shear [16–18] and extension [19,20]. Other effects of LCB are increased zero shear viscosity η_0 accompanied by increased shear thinning [14,17–19,21–23] when linear and long chain branched materials with similar MWD are compared. Increased flow activation energy is another effect observed in this connection [17,20,22,24]. These effects can be observed at very low LCB contents. For example Yan et al. [25] have reported η_0 enhancement at content as low as 0.2 LCB/10000 C. This makes rheometry a very sensitive method for LCB detection. Unfortunately for the detection of LCB the effect mentioned above can also be a result of a broadened MWD. It is important to note that the findings referred to above are for polyethylene with a few long branches. LDPE is often referred to as the traditional LCB-PE but for this material η_0 and the elasticity in shear can be lower than linear materials with similar MWD [18]. This is due to compact dendritic structure of LDPE.

A feature of LCB that is not found in linear materials is thermorheological complexity. Polymers for which the time temperature superposition principle is valid is said to be thermorheological simple. This class includes linear and short chain branched polymers. Due to their complex relaxation pattern the time temperature principle is not valid for LCB polymers and they are said to be thermorheological complex [26]. Mavridis and Shroff [24] have shown that a plot of the logarithm of the loss tangent $\tan\delta = G''/G'$ versus the logarithm of the complex modulus G^* at different temperature can verify whether a polymer is thermorheologically simple or complex. In this plot data from different temperatures will superimpose in the case of thermorheological simplicity but not in the case of thermorheological complexity. A variant of this plot where the phase angle δ is plotted versus modulus has been studied in details by Trinkle et al. [27,28].

1.4. Size exclusion chromatography

Size exclusion chromatography (SEC) is the primary method for determination of MWD [29]. If equipped with a viscosity detector (VD) in addition to the concentration detector SEC can also be used for branching analysis. From the concentration and the VD signal the intrinsic viscosity $[\eta]$ of each eluting fraction can be determined. $[\eta]$ is a measure of specific volume in solution and it is related to the molecular weight and the hydrodynamic volume through the equation [30,31].

$$V_h \propto M[\eta] \tag{4}$$

In SEC a certain V_h corresponds to a certain retention volume V_e. Thus, M is found from the measured $[\eta]$ and a calibration curve of Log $M[\eta]$ as a function of V_e. The fundament for the branching analysis were established by Zimm and Stockmayer [32]. Based on the fact that branched chains are denser than linear chains of the same M they derived relations between branching densities and the contraction factor g defined as

$$g = \left(\frac{\langle R_g^2\rangle_{br}}{\langle R_g^2\rangle_{lin}}\right)_M \tag{5}$$

where $\langle R_g^2\rangle$ is the mean square radius of gyration. g' is corresponding factor involving $[\eta]$, defined as

$$g'\left(\frac{[\eta]_{br}}{[\eta]_{lin}}\right)_M \tag{6}$$

g and g' are related as

$$g' = g^{\varepsilon} \tag{7}$$

The factor ε is reported to take values between approximately 0.5 and 1.5 [33–35]. Based on values recently reported [33] for PE of similar MWD and branching content as we expect, we decided to use $\varepsilon = 1.5$. We expect 1,3-BDSA to form four functional random cross-links. For that case Zimm and Stockmayer [32] found

$$g = \left[\left(1 + \frac{\beta}{6}\right)^{1/2} + \frac{4\beta}{3\pi}\right]^{-1/2} \tag{8}$$

where β is the number of branch points per molecule. Branching frequencies per 10,000 carbon λ are determined as

$$\lambda = \frac{\beta \times 140,000}{M} \tag{9}$$

2. Experimental

2.1. Materials

Metallocene HDPE homopolymer from now on referred to as PE1 was supplied by Borealis AS as unstabilized reactor powder. (1,3-BDSA) was synthesised as described earlier [10] PE1 was stabilized with 600 ppm Irganox 1010, 1200 ppm Irgafos 168 and 900 ppm zinc stearate. The stabilizers were supplied by Ciba Specialty Chemicals Inc.

2.2. Cross-linking procedure

PE1 was modified at concentrations of 0, 16, 128, 257, 512 and 1027 ppm 1,3-BDSA. From elementary stoichiometric calculations one finds that 1 ppm of 1,3-BDSA corresponds to 0.0005 1,3-BDSA/10,000 carbon. The number of 1,3-

BDSA/10,000 carbon for the respective samples are listed in Table 3.

The cross-linking was carried out by reactive extrusion at 200 °C. The steps of the cross-linking procedure were the following: an accurate amount of 1,3-disulfonyl-azidobenzene was dissolved in 5 ml of acetone. After dissolution another 5 ml of acetone was added to the solution to give a 10 ml solution. The solution was added to 500 g PE1 powder and blended thoroughly into the powder. After evaporation of the acetone the blend was extruded. We used a Clextral co-rotating twin-screw extruder BC21 with screw diameter 25 mm and screw length 80 cm. The extruder operated at 100 rpm and was fed at a rate of 30 g/min. To obtain an even distribution of the cross-linker the extruder was divided into different temperature zones. The first zones were at low temperature to ensure good blending before cross-linking took place. The residence time in the extruder were determined to be from approximately two to four minutes. This was done by adding carbon black at a specific time and measuring its passage time. As seen from Table 1 the residence time is possibly not long enough to obtain a full conversion of all 1,3-BDSA. Anyway this was not a problem since the products, before all measurements, were melted and formed at 200 °C. Thus, the total time at 200 °C in all cases exceeded 4 min.

2.3. Gel analysis

The most modified sample was examined for content of gel after ASTM 2765 'Determination of gel content and swell ratio of cross-linked ethylene plastics'. The basis of this standard is extraction in boiling para-xylene.

2.4. Melt index

Melt index were measured after ASTM D 1238 (2.16 kg, 190 °C).

2.5. Density

Densities were measured in a density column after ASTM D 1505. The cross-linking reaction generates N_2 that forms gas bubbles that disturb density measurements. For this reason density measurements were done on strings from the melt index capillary.

2.6. Size exclusion chromatography

Size exclusion chromatography analyses were performed using a Polymer Laboratories GPC 210 equipped with a PL differential refractometer (DRI), a two angle (15 and 90°) Precision Detector PD2040 light scattering detector (LSD) (not in use), and a Viscotec 150R differential bridge viscometer detector (VD). All detectors were situated in the oven compartment. The LSD was placed immediately after the columns followed by the DRI and the VD in parallel with an approximately 50:50 flow split. The columns used were a set of four Plgel 20 μm MIXED-A LS 300×7.5 mm and a Plgel 20 μm Guard 300×7.5 mm. The analyses were performed at 145 °C with a flow rate of 1.00 mL/min and 1,2,4-trichlorobenzene (TCB) stabilized with 0.02 wt% 2,6-Di-tert-butyl-p-cresol (BHT) as solvent. The columns and the detectors were calibrated using 14 narrow polystyrene (PS) standards supplied by Polymer Laboratories with molecular weights ranging from 600 to 2×10^6. A 200 μm injection loop was used for all measurements. Universal calibration was used for the determination of molecular weight from the DRI and the VD signal. The performance of the VD was validated from the Mark–Houwink constants obtained for PS from the universal calibration. The values obtained were $a=0.665$ and $K=1.6\times10^{-4}$ mL/g. These are in agreement with values reported in the literature $a=0.670$ and $K=1.75\times10^{-4}$ mL/g. Samples for SEC were prepared by dissolving an accurate amount of approximately 20 mg sample in 20 mL of 1,2,4-trichlorobenzene (TCB) stabilized with 0.02 wt% BHT. Dissolution of the samples was achieved in an oven at 160 for 1.5 h. To minimise dissolution time and thereby degradation the sample surface areas were maximised by pressing the pellets to thin films and cutting the film in threads. The films were made by melting the samples at 200 °C and after that gradually pressing the samples to films. A motorised press was used in this operation. The total time at 200 °C was 90 s. Rheology tests showed that the samples are stable for periods much longer than this.

PE1 contains residues of catalyst particles. To avoid column frit blockage (10 μm column frit) from these particles all samples where filtered at 145 °C with a hot filtration device consisting of a syringe and filter in a heated block. The filters used were 5 μm MITEX PTFE discs from Millipore contained in a Swinney Stainless Filter Holder.

2.7. Rheometry

Dynamic mechanical analysis and creep measurements were done with a DSR200 from Rheometrics Scientific using parallel plate geometry with 25 mm diameter. The separation between the parallel plates was 2 mm. Samples were prepared by pressing pellets in a form at 200 °C.

3. Results and discussion

The density analysis was not able to distinguish between the samples. The densities were randomly distributed around 0.947 ± 0.001. We, therefore, expect the crystallinity to be unaffected by the processing. Gel content analysis of the most modified sample (1027 ppm) revealed zero gel content.

3.1. SEC

Fig. 2 shows the molecular weight distributions. As expected the results of the cross-linking is a slight broadening of the MWD due to the formation of a high molecular weight fraction. The changes in MWD are small and are easier seen when the high molecular tails are enlarged as in Fig. 3. The high molecular fraction increases continuously with the amount of 1,3-BDSA used and becomes clearly evident for

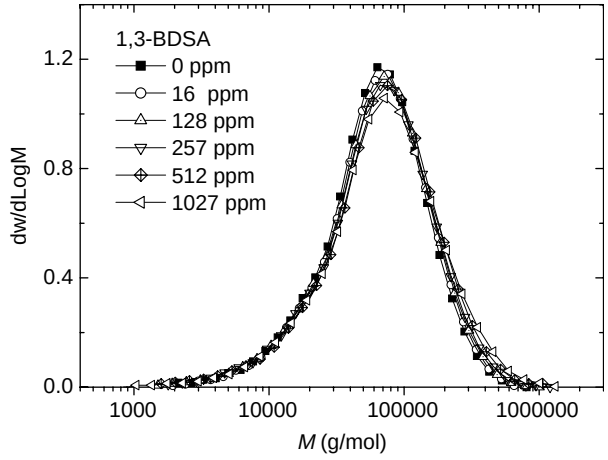

Fig. 2. Molecular weight distributions of linear polyethylene lightly cross-linked with varying amounts of 1,3-BDSA.

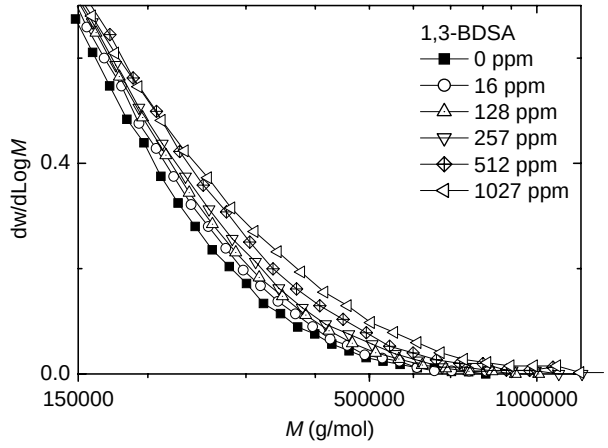

Fig. 3. High molecular weight tail of linear polyethylene lightly cross-linked with varying amounts of 1,3-BDSA.

concentrations above 500 ppm. Notably there are no signs of formation of a low molecular fraction due to chain scission. The molecular weight averages are listed in Table 2. In Fig. 4 the intrinsic viscosity is plotted as a function of the molecular weight (Mark–Houwink plot). Here, we see that $[\eta]$ in the high molecular weight fraction decreases continuously with increased amount of 1,3-BDSA. The decrease is not large, but earlier studies [21] have shown that for such sparse levels of branching as we expect, the change in $[\eta]$ will be at the limit of detection. Branching numbers β and branching density λ as a function of molecular weight are shown in Figs. 5 and 6, respectively. Both of these dataset are relatively uncertain since they rely on the small differences of the data in Fig. 4. As expected β and λ increase with 1,3-BDSA concentration. With an even distribution of cross-links, we expect $\lambda(M)$ to be constant. However, in our results it passes through a maximum. This could be a result of our assumption of a constant $\varepsilon = 1.5$. ε is theoretically expected and has been reported to decrease with decreasing g and g′ [34,35]. A decrease in ε with g' would for our data lead to a higher λ in the high molecular fraction

Table 2
Weight and number average results from SEC analyses

[1,3-BDSA] (ppm)	[1,3-BDSA] /10^4 carbon	M_n g/mol × 10^{-3}	M_w g/mol × 10^{-3}	PD	g'_n	g'_w	g_n	g_w	λ_n (branch points/10^4 carbon)	λ_w (branch points/10^4 carbon)	β_n (branch points molecule)	β_w (branch points molecule)
0	0	40 ± 1	82 ± 1	2.1								
16	0.008	45 ± 3	85 ± 2	1.9								
128	0.062	42 ± 2	89 ± 2	2.1	0.997	0.981	0.997	0.988	0	0.034	0.018	0.063
257	0.125	40 ± 1	91 ± 3	2.3	0.990	0.976	0.993	0.984	0	0.09	0.035	0.080
512	0.249	42 ± 1	96 ± 2	2.3	0.978	0.963	0.985	0.976	0.008	0.13	0.068	0.12
1027	0.500	42 ± 2	104 ± 3	2.5	0.951	0.924	0.967	0.949	0.20	0.32	0.15	0.24

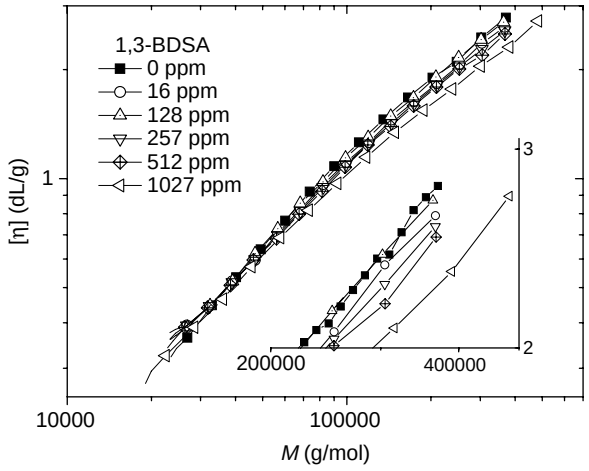

Fig. 4. Intrinsic viscosity [η] as a function of molecular weight M of linear polyethylene lightly cross-linked with varying amounts of 1,3-BDSA. The insert shows an enlargement of the high molecular weight region data.

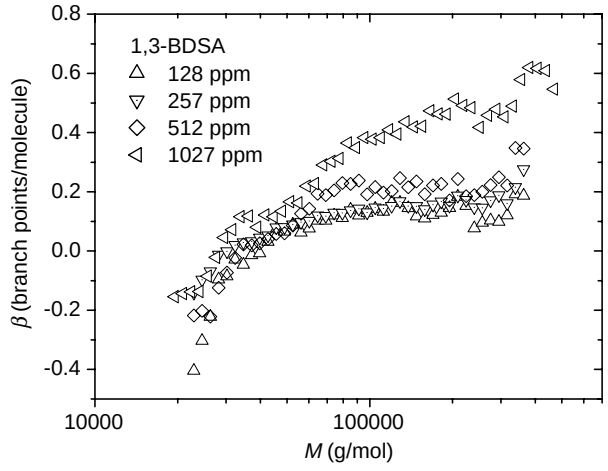

Fig. 5. Branching number β of linear polyethylene lightly cross-linked with varying amounts of 1,3-BDSA.

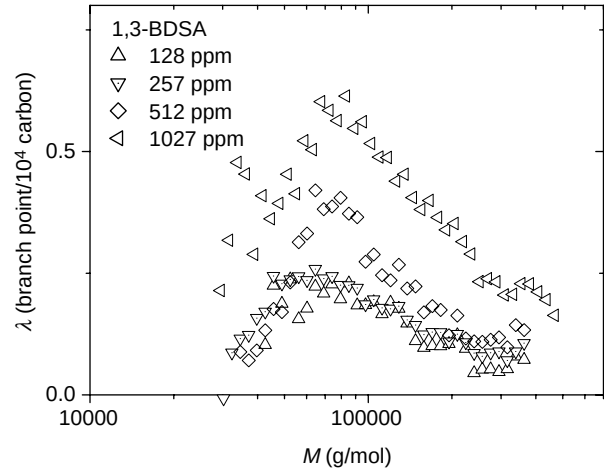

Fig. 6. Branching frequency α of linear polyethylene lightly cross-linked with varying amounts of 1,3-BDSA.

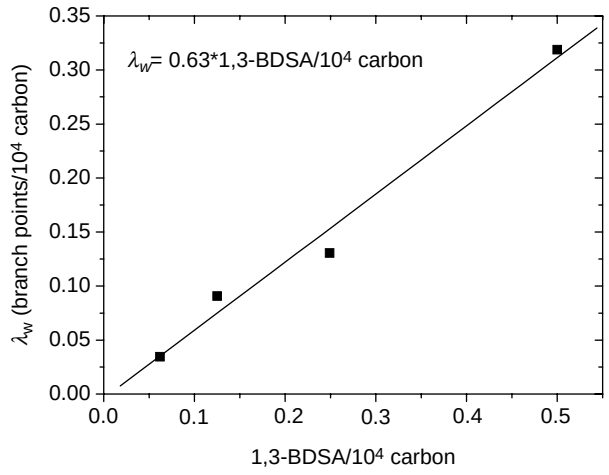

Fig. 7. Molecular weight average branching frequency λ_w as a function of cross-linker fraction (1,3-BDSA/10^4 carbon).

than shown in Fig. 6. Number and weight averages of the parameters obtained in the SEC analysis are listed in Table 2.

Fig. 7 shows the molecular weight average branching frequency λ_w as a function of cross-linker fraction (1,3-BDSA/10^4 carbon). For a 100% effective cross-linking process we expect those two parameters to be equal. From a nicely fitting least squares linear fit we find a cross-linking efficiency of 63%. Another way to estimate the efficiency of 1,3-BDSA is to compare the measured M_w with those predicted from random cross-linking theory (Eq. (1)). This is done in Fig. 8. The M_w growth predicted with a 100% efficient cross-linker ($\nu = 1$) strongly exceeds the measured M_w. The best fit of the theory is obtained with a cross-linking efficiency of 40% ($\nu = 0.4$). Considering the nature and assumptions of the models used and the accuracy of the data this difference in efficiency is not dramatic. Also, consider for example how an intra-chain cross-linked polymer chain is interpreted by the two models. Intra-chain cross-linking would not affect the molecular weight. However, intrachain cross-linking can result in loops that resembles LCB or other structures that prevent the chain from expanding in a good

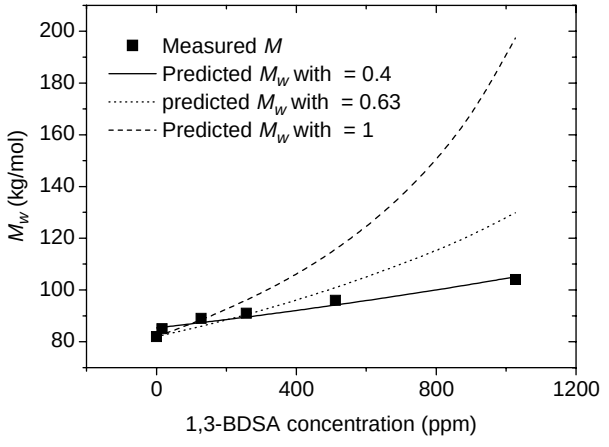

Fig. 8. Growth of M_w with increasing amount of cross-linking as measured by SEC and as predicted from theory of random cross-linking [13]. The theoretical values are predicted from Eqs. (1) and (3). ν is the efficiency of the cross-linker.

solvent and thereby reduce [η] of the chain (1,2,4-TCB used in the SEC analysis is a good solvent for PE). In that case, the intra-chain cross-link would increase the cross-linking density as evaluated by the LCB and cross-link analysis involving g'. On the other hand, since the molecular weight is unchanged the intra-chain cross-link would not be considered when evaluating the cross-linking density with the random cross-linking model. This is one possible reason for the difference in results obtained from the two methods.

The 1,3-BDSA not involved in cross-linking must be accounted for in other ways. The most likely destiny is intra-chain cross-linking, double cross-linking of the same chains, or unwanted reactions such as dimerization or oxidation of sulfonyl nitrenes [10,12]. Mechanical chain or cross-link cleavage during extrusion will also reduce the apparent efficiency. Intra-chain cross-linking will always occur. Double cross-linking and dimerization can be reduced with improved blending. Oxidation is limited by processing in an inert atmosphere. Thus, there are ways to improve the efficiency.

We conclude that the SEC data support that modification with 1,3-BDSA has introduced a long chain, branched, high molecular weight fraction and that no chain scission has occurred. The SEC analyses suggest that the efficiency of 1.3-BDSA to form cross-links in the actual process is in the range of 40–60%. We do not observe any very high molecular weight tail in the MWD and the branching numbers β are well below one in the whole molecular weight range. This supports the hypothesis that 1,3-BDSA is evenly distributed in the polymer

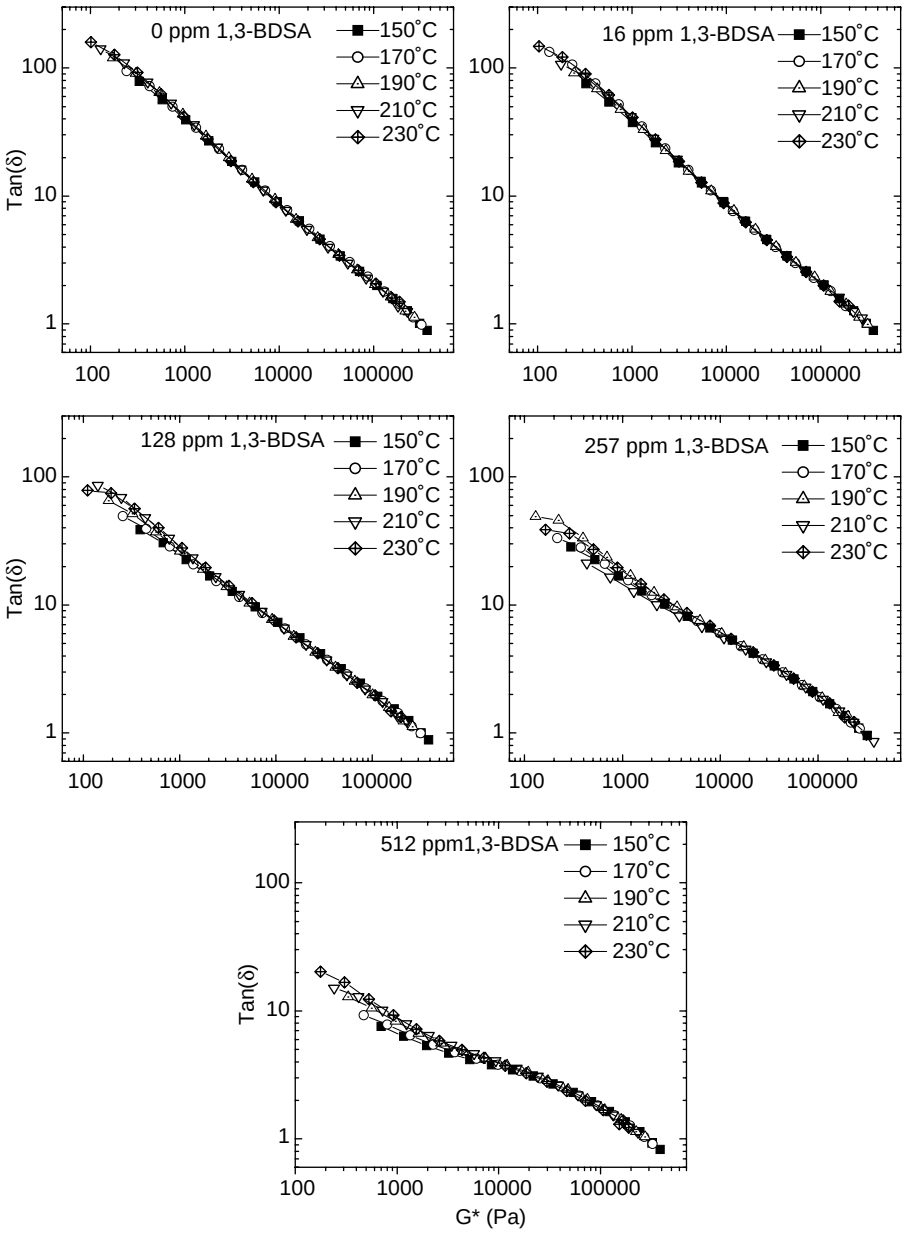

Fig. 9. Tan δ versus G^* plot for 0, 16, 128, 257 and 512 ppm of the cross-linker 1,3-BDSA. Increasing lack of superposition indicates increasing thermorheological complexity.

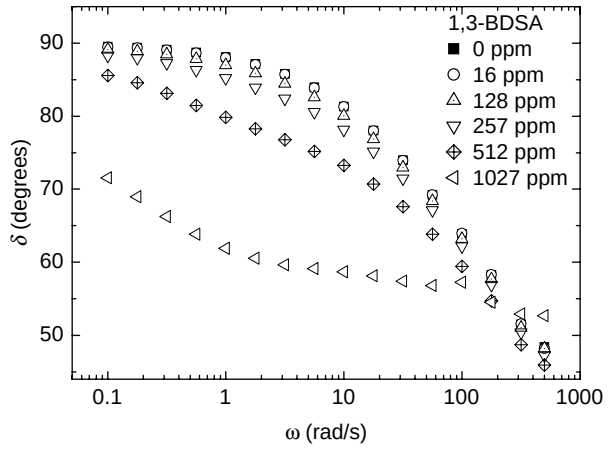

Fig. 10. Evolution of the phase angel at 190 °C with increasing amount of cross-linking.

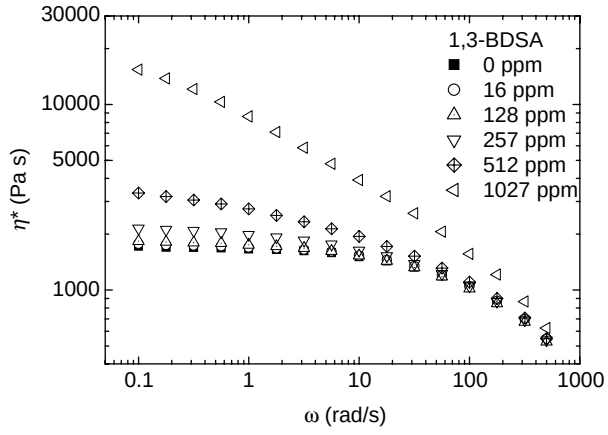

Fig. 11. Evolution of the complex viscosity at 190 °C with increasing amount of cross–linking.

and that cross-linking in most cases lead to simple structures such as four armed stars.

3.2. Rheology

Rheological measurements where made on all the samples described but the most modified (1027 ppm) sample was challenging to work with. In the case of creep measurements, steady state was not fully reached for this sample within a time period where degradation could be discounted, and increasing the stress lead to non-linear behavior. In the case of dynamic mechanical analysis reliable data were not obtained in the whole frequency and temperature range used. These problems could possible be caused by insufficient adhesion of the sample to the plates. As a result dynamic data for the 1027 ppm 1,3-BDSA sample are omitted in parts of the discussion below.

Results from dynamic mechanical analyses at the temperatures 150, 170, 190, 210 and 230 °C are presented in different forms in Figs. 9–11. Fig. 9 shows plots of tan δ versus G^* data for samples with 0, 16, 128, 257 and 512 ppm 1,3-BSDA at the five temperatures considered. This plot series gives a good view of the evolution of a thermorheological complex structure with increasing cross-linking. Data from samples without cross-linking at all temperatures superimpose indicating a linear structure. With increasing cross-linking a deviation between the data at different temperatures appears and the deviation increases continually with the amount of cross-linking. The thermorheological complexity is most evident at low frequency, while at high frequencies there is good superposition in all cases, and the properties are independent of the cross-linking. Low frequencies probe relaxations at relatively large spatial dimensions in the structure and high frequencies correspond to relatively short distances. Thus, the data tells us that the cross-linking has not altered the relaxation behavior at short distances. This is in good agreement with what we expected, namely formation of branches of a length comparable with the main chain. This interpretation also agrees with result on classical LDPE [24] and peroxide modified linear chains [36]. In the case of LDPE a lack of superposition is seen in a broad frequency range. This is in accordance with the random structure of LDPE with branching on all scales. An LLDPE treated with 150 ppm peroxide showed behavior similar to that observed in this work [36].

It is also worth to note that the samples start to behave more like a network as the cross-linking increases. In the phase angle plot Fig. 10 this is seen through the formation of a plateau. Fig. 11 shows the complex viscosity as a function of frequency. Here we see a clear viscosity enhancement at low deformation rate with increasing cross-linking. The increased viscosity at low rate is accompanied by and increased shear thinning. As discussed above this effect could also be a result of a broadening of the MWD without LCB but in the cases considered here the MWD's are so similar that we assign it to the presence of LCB. Zero shear viscosities η_o were estimated as the steady state viscosity in creep measurements at 190 °C.

Table 3
Characteristics of PE cross-linked with 1,3-BDSA

[1,3-BDSA] (ppm)	M_w (g/mol$\times 10^{-3}$)	λ_n (branch points/10^4 carbon)	λ_w (branch points/10^4 carbon)	β_n (branch points / molecule)	β_w (branch points / molecule)	η_o (kPa s)	J_e^0 (Pa$^{-1}\times 10^{-4}$)	σ_{creep} (Pa)	MI(190 °C 2.16 kg) (g/min)
0	82±1					2.4±0.05	3±2	3	4.1
16	85±2					2.4±0.05	2±2	3	4.0
128	89±2	0	0.034	0.018	0.063	2.8±0.1	24±9	6	3.8
257	91±3	0	0.09	0.035	0.080	3.4±0.1	69±9	12	3.2
512	96±2	0.008	0.13	0.068	0.12	6.3±0.2	126±4	24	2.4
1027	104±3	0.20	0.32	0.15	0.24	45±3	101±19	24	0.8

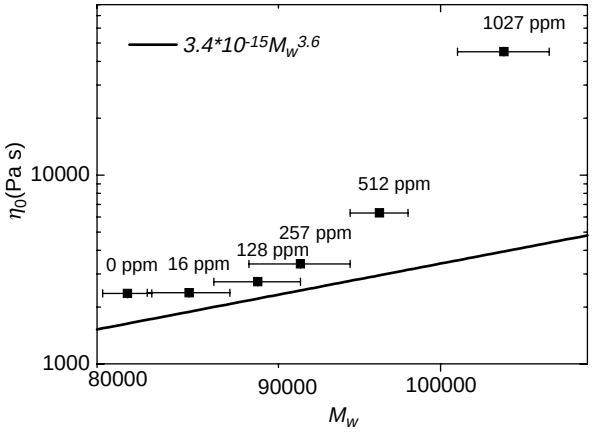

Fig. 12. Molecular weight dependence of the zero shear viscosity at 190 °C for linear polyethylene cross-linked with 0–1027 ppm 1,3-BDSA. The solid line represent the relation between zero viscosity and molecular weight for linear PE [37]: $\eta_0 = 3.4 \times 10^{-15} M_w^{3.6}$.

The steady state compliances J_e^0 were determined from the same data. The steady state viscosity was determined from the slope of the tangent of $J(t)$ at steady state. J_e^0 was determined from the intercept of the same slope with the ordinate. There were large differences in the time and deformation to obtain steady state. To avoid thermal decomposition due to long measurement time, increasing stress was applied with increasing cross-linking. The shear stresses applied σ_{creep} are listed in Table 3 together with the results. Fig. 12 shows the zero shear viscosity found from creep measurements as a function of the weight average molecular weight found with SEC. The viscosity values are a little higher than the complex viscosities found at the lowest frequencies but the ratios of the values from the different samples are nearly equal. A study by Raju et al. [37] resulted in a formula that is generally accepted as the standard relation between molecular weight and zero shear viscosity for PE. The relation is

$$\eta_0 = 3.4 \times 10^{-15} M_w^{3.6} \quad (10)$$

A line of this form is drawn together with our data. The viscosity values we have obtained for linear unmodified

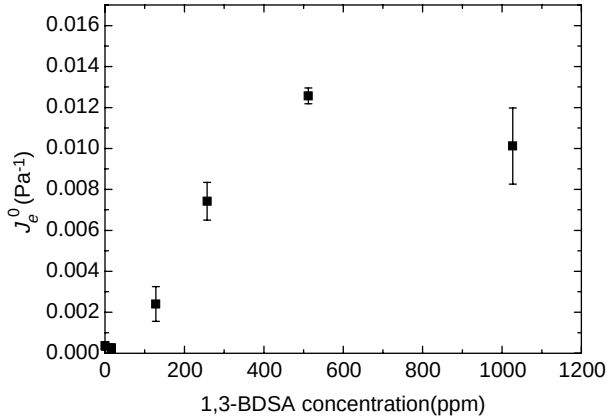

Fig. 13. Dependence of the creep recovery compliance at 190 °C on the amount of cross-linker 1,3-BDSA.

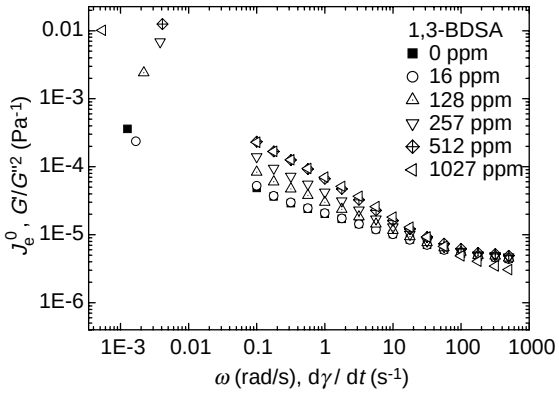

Fig. 14. G'/G''^2 vs. angular frequency ω and J_e^0 vs. creep strain rate $d\gamma/dt$ at 190 °C.

polyethylene is close to this line and do not increase considerably for concentrations of 1,3-BDSA up to 257 ppm. When the amount of cross-linking increases further the viscosity deviates strongly upwards. This is what we expect when LCB are present.

The steady state compliances are presented in Fig. 13 and listed in Table 3. The effect on compliance is more pronounced for small levels of cross-linking than for viscosity. J_e^0 increases from 3 to 126 $Pa^{-1} \times 10^{-4}$ when the amount of 1,3-BDSA is increased from 0 to 512 ppm but then decreases when the concentration is increased to 1027 ppm. This decrease is surprising but is supported by plots of G'/G''^2 versus frequency (Fig. 14). Such plots will, due to linear viscoelastic theory [38], tend towards J_e^0 as the frequency goes towards zero. G'/G''^2 increases with increasing cross-linking up to 512 ppm 1,3-BDSA but does not increase further for 1027 ppm. The G'/G''^2 data as a function of frequency for 1027 ppm data also shows a slight downwards curvature at low frequencies while the 512 ppm data are more linear. This suggests that G'/G''^2 is lower for 1027 ppm than for 512 ppm at frequencies below our measurement interval. A possible explanation for the observed development of J_e^0 is discussed below.

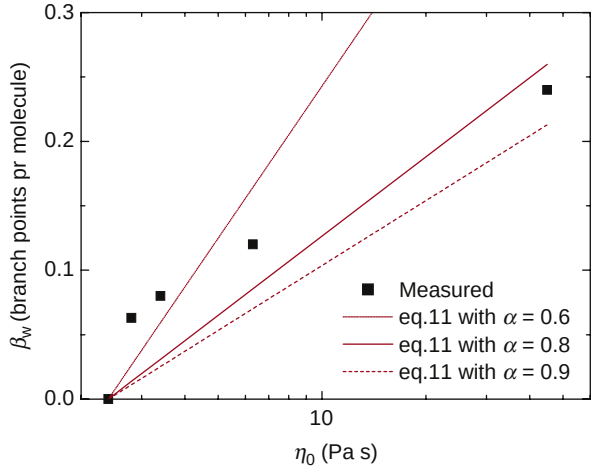

Fig. 15. Comparison of measured β_w values with those predicted by the theory of Gotsis et al. (Eq. (11)). $M_c = 3000$ g/mol. The best fit in a least squares sense is obtained with $\alpha = 0.8$.

It is interesting to explore whether our data can infer more about the structure in our cross-linked samples than that they contain LCB. A guide to this can possibly be found in a comprehensive study by Lohse et al. [22]. They investigated how the chain structure affects the rheology of polymers. This was done with a large number of samples with different very well-defined structures (stars, combs, H's). They found for blends of symmetric stars and linear chains only a slight increase in viscosity when the linear part dominates followed by a strong increase when the star geometry starts to dominate. In contrast to this the shear recovery compliance of these blends increased significantly for only small fraction of stars and then decreased. Similar behavior was observed by Liau et al. [39]. In other words, a blend of linear and star polymers can actually posses higher J_e^0 than the pure components. This behavior is similar to what we observe in our cross-linked samples. As discussed earlier in this paper, blends of linear and star-shaped molecules with increasing fraction of stars with increasing cross-linking are a likely result of the procedure we have used. An explanation for the observed J_e^0 development can, therefore, be that our sample series vary over a region where the dominant shape changes from linear to star. Surely the branches generated by cross-linking will never be as regular as those found in the model blends referred to above, but the similarity in properties is still interesting.

Gotsis et al. have performed studies similar to this work [40–42]. Their work considers light cross-linking of PP and the consequence of this on rheological properties. They have developed a simple theory relating η_0 to the degree of branching [42]. The theory assumes that for low levels of cross-linking the number of branch points pr molecule β is either zero or one, and that the polymer material consist of a fraction $(1-x)$ of linear chains and a fraction x of stars with arm length half of the average length of the linear precursor. It is easy to show that under these assumptions the fraction of branched molecules x equals the weight average number of branch points pr molecule β_w. The theory of Gotsis et al. is expressed through the formula

$$\beta_w = \frac{\ln\left\{\frac{\eta_0^{BL}}{\eta_0^{L}}\right\}}{\alpha\left[\left(\frac{M_L}{M_C}\right)-1\right]-3\ln\left\{\frac{M_L}{M_C}\right\}} \tag{11}$$

Here η_0^{BL} and η_0^{L} are the zero shear viscosity of the linear-star blend and the linear precursor, respectively. α is a constant. Molecular theory predicts $\alpha = 15/8$, but experiments suggest $\alpha \approx 0.4-0.6$ [42]. M_L is the molecular weight of the linear precursor and M_c is the critical entanglement molecular weight. Note that the denominator in Eq. (11) is a constant so the predicted β_w is a linear function of ln η_0 that crosses the abscissa at η_0^L. Gotsis et al. found good correlation of SEC and rheometry results through Eq. (11). We like to test whether it is valid for our data. As Gotsis et al. we assume $M_c = 2M_e$. The molecular weight between entanglements M_e for PE has been reported to be approximately 1500 g/mol [37,43]. We, therefore, use $M_c = 3000$ g/mol. Fig. 15 shows the measured β_w and values calculated with different α values. The measured β_w values are not linear dependent on ln η_0 so the model is not able to describe them. The best fit in a least squares sense is obtained with $\alpha = 0.8$. Based on these few data it is difficult to judge the reliability of the model. The results are highly dependent on α, so the use of the model to measure the degree of branching requires that the value of α is more clarified.

4. Conclusions

Analysis with SEC and rheometry has shown that reactive extrusion of polyethylene with small amounts of 1,3 benzenedisulfonyl azide at 200 °C leads to the formation of long chain branches. No signs of formation of low molecular species could be observed with SEC thereby suggesting that radical reactions leading to chain scission are negligible. From comparison with theory of random cross-linking and traditional SEC-LCB analysis we estimated the cross-linking efficiency of 1,3-BDSA in our process to be 40–60%. The rheological tests also supported the formation of long chain branches. This was seen through the appearance of thermorheological complexity and strongly increased viscosity combined with increased shear thinning and increased melt elasticity. These rheological changes associated with LCB became evident after cross-linking with concentrations of 1,3-bezenedisulfonyl benzene above approximately 100 ppm. 100 ppm corresponds to approximately 0.05 1,3-BDSA/10^4 carbon (basic stoichiometry). This again corresponds to approximately 0.03 branch points/10^4 carbon (Fig. 7). The data thereby emphasize the strong impact of LCB on melt flow behaviour.

The recovery compliance increased to a maximum at cross-linking with 500 ppm 1,3-BDSA but then decreased when the cross-linker concentration was increased to 1027 ppm. We proposed that this could be due to the transitions from linear chains to a blend dominated by stars. The SEC and rheology analyses support the hypotheses that 1,3-BDSA can be evenly distributed in the polymer and that formation of simple branching structures such as four armed stars are a likely result of the cross-linking process.

Acknowledgements

The authors thank Borealis AS and The Research Council of Norway for financing this work. We also thank Dr Erik Andreassen for assistance with rheometry.

References

[1] Breslow DS, Spurlin HM. US Pat. 3203937; 1965.
[2] Terbrueggen RH, Drumright RE. World Pat. 2000052091; 2000.
[3] Machado MAL, Kenny JM. Rubber Chem Tech 2001;74:198–210.
[4] Benito Gonzalez JL, Ibarra Rueda LM, Gonzalez Hernandez L. Kautsch Gummi Kunstst 1990;43:697–700.
[5] Gonzalez Hernandez L, Rodriguez Diaz A, De Benito Gonzalez JL. Rubber Chem Tech 1992;65:869–78.
[6] Andreassen E, Borve KL, Rommetveit K, Redford K. Annu Tech Conf - Soc Plast Eng 1999;57th:2104–8.
[7] Borve KL, Redford K, Skattum M, Haavaldsen JT. World Pat. 2001066632; 2001.

[8] Breslow DS, Sloan MF, Newburg NR, Renfrow WB. J Am Chem Soc 1969;91:2273–9.
[9] Lwowski W. Nitrenes, New York: John Wiley and Sons inc., 1970.
[10] Jørgensen JK, Stori A, Redford K. Polymer 2005; accepted, doi:10.1016/j polymer. 2005.10.077
[11] Reiser A, Leyshon LJ, Johnston L. Trans Faraday Soc 1971;67:2389–96.
[12] Yasuda N, Yamamoto S, Wada Y, Shozo Y. J Polym Sci, Polym Chem 2001;39:4196–205.
[13] Macosko CW, Miller DR. Macromolecules 1976;9:199–206.
[14] Bubeck RA. Mat Sci Eng R 2002;39:1–28.
[15] McLeish TCB. Curr Opin Solid State Mater Sci 1997;2:678–82.
[16] Gell CB, Graessley WW, Efstratiadis V, Pitsikalis M, Hadjichristidis N. J Appl Polym Sci 1997;35:1943–54.
[17] Gabriel C, Munstedt H. Rheol Acta 1999;38:393–403.
[18] Gabriel C, Munstedt H. Rheol Acta 2002;41:232–44.
[19] Bin Wadud SE, Baird DG. J Rheol 2000;44:1151–67.
[20] Malmberg A, Gabriel C, Steffl T, Munstedt H, Loefgren B. Macromolecules 2002;35:1038–48.
[21] Wood-Adams PM, Dealy JM, deGroot WA, Redwine DO. Macromolecules 2000;33:7489–99.
[22] Lohse DJ, Milner ST, Fetters LJ, Xenidou M, Hadjichristidis N, Mendelson RA, et al. Macromolecules 2002;35:3066–75.
[23] Gabriel C, Kokko E, Lofgren B, Seppala J, Munstedt H. Polymer 2002;43:6383–90.
[24] Mavridis H, Shroff RN. Polym Eng Sci 1992;32:1778–91.
[25] Yan D, Wang WD, Zhu S. Polymer 1999;40:1737–44.
[26] Graessley WW. Macromolecules 1982;15:1164–7.
[27] Trinkle S, Friedrich C. Rheol Acta 2001;40:322–8.
[28] Trinkle S, Walter P, Friedrich C. Rheol Acta 2002;41:103–13.
[29] Yau WW, Kirkland JJ, Bly DD. Modern size exclusion chromatography. New York: Wiley; 1979.
[30] Grubisic Z, Rempp P, Benoit H. J Polym Sci, Phys Ed 1996;34:1707–13.
[31] Grubisic Z, Rempp P, Benoit H. Polym Lett 1967;5:753–9.
[32] Zimm BH, Stockmayer WH. J Chem Phys 1949;17:1301–14.
[33] Wang WJ, Kharchenko S, Migler K, Zhu S. Polymer 2004;45:6495–505.
[34] Tackx P, Tacx JCJF. Polymer 1998;39:3109–13.
[35] Beer F, Capaccio G, Rose LJ. J Appl Polym Sci 2001;80:2815–22.
[36] Shroff RN, Mavridis H. Macromolecules 1999;32:8454–64.
[37] Raju VR, Smith GG, Marin G, Knox JR, Graessley WW. J Polym Sci, Phys Ed 1979;17:1183–95.
[38] Ferry JD. Viscoelastic properties of polymers. 3rd ed. New York: Wiley; 1980.
[39] Liau WB, Uen JS, Chiu WY. Eur Polym J 1998;36:101–9.
[40] Gotsis AD, Zeevenhoven BLF, Tsenoglou C. J Rheol 2004;48:895–914.
[41] Lagendijk RP, Hogt AH, Buijtenhuijs A, Gotsis AD. Polymer 2001;42:10035–43.
[42] Tsenoglou CJ, Gotsis AD. Macromolecules 2001;34:4685–7.
[43] Raju VR, Rachapudy H, Grassley WW. J Polym Sci Phys Ed 1979;17:1223–35.